

Beyond Model Design: Data-Centric Training and Self-Ensemble for Gaussian Color Image Denoising

Gengjia Chang¹ Xining Ge² Weijun Yuan³ Zhan Li³

Qirong Song⁴ Luen Zhu⁵ Shuhong Liu^{6,†}

¹Hefei University of Technology ²Hangzhou Dianzi University ³Jinan University

⁴South China Agricultural University ⁵The University of Tokyo

Abstract

This paper presents our solution to the NTIRE 2026 Image Denoising Challenge (Gaussian color image denoising at fixed noise level $\sigma = 50$). Rather than proposing a new restoration backbone, we revisit the performance boundary of the mature Restormer architecture from two complementary directions: stronger data-centric training and more complete Test-Time capability release. Starting from the public Restormer $\sigma = 50$ baseline, we expand the standard multi-dataset training recipe with larger and more diverse public image corpora and organize optimization into two stages. At inference, we apply $\times 8$ geometric self-ensemble to further release model capacity. A TLC-style local inference wrapper is retained for implementation consistency; however, systematic ablation reveals its quantitative contribution to be negligible in this setting. On the challenge validation set of 100 images, our final submission achieves 30.762 dB PSNR and 0.861 SSIM, improving over the public Restormer $\sigma = 50$ pretrained baseline by up to 3.366 dB PSNR. Ablation studies confirm that the dominant gain originates from the expanded training corpus and the two-stage optimization schedule, while self-ensemble provides a small but consistent additional boost.

1. Introduction

Image denoising is a fundamental low-level vision task that underpins a broad spectrum of downstream applications, including image restoration [27, 56], autonomous driving [38, 48, 73], VR/AR [37], 3D reconstruction [23, 45, 50], scene understanding [46, 47, 49], and scientific discovery [49]. For Gaussian color image denoising at a fixed noise level, deep learning has already established a mature technical spectrum. Representative CNN-based methods such as

DnCNN [70], FFDNet [71], and RIDNet [7] demonstrate that residual learning, noise-aware conditioning, and feature attention can substantially improve restoration quality. Multi-stage restoration frameworks such as MPRNet [66] further show that progressive refinement can be as consequential as raw backbone capacity.

Transformer-based approaches have pushed this frontier further. SwinIR [41], Uformer [62], and Restormer [63] establish that long-range dependency modeling and efficient multi-scale feature interaction are highly effective for image restoration. Among these, Restormer has emerged as a particularly strong public baseline for high-resolution restoration and Gaussian denoising, owing to its favorable balance between global context modeling and computational practicality. Once a backbone of this caliber is in place, however, the remaining performance gap may no longer be primarily attributable to architectural limitations. Instead, the binding constraint may shift to how much statistical prior the training corpus can inject into the model, and to what extent the inference strategy can fully exploit what a well-trained checkpoint already encodes.

Motivated by this observation, we investigate how far a mature Restormer denoiser can be pushed through two complementary and practically accessible levers. On the training side, we expand the corpus beyond the standard public recipe and organize optimization into two successive stages, allowing stronger checkpoints to emerge from greater visual diversity and more stable convergence. On the inference side, we apply $\times 8$ geometric self-ensemble to aggregate predictions across all symmetries of the dihedral group, yielding a more stable and consistent final output. A TLC-style local inference wrapper is retained in our implementation for consistency with prior practice, but systematic ablation shows that its quantitative contribution in this setting is negligible. Our experimental protocol is therefore explicitly designed to isolate what genuinely drives performance from what merely persists in the engineering pipeline.

The main contributions of this work are as follows. First, we demonstrate that a Restormer-based Gaussian de-

The NTIRE 2026 Image Denoising Challenge (noise level=50) is hosted on Codabench. Official page: <https://www.codabench.org/competitions/12905/>.

noiser can be substantially improved without any architectural modification, through corpus expansion and a two-stage training schedule alone. Second, we provide a systematic quantification of the gain attributable to $\times 8$ geometric self-ensemble at inference, along with its associated computational overhead. Third, through controlled comparison against the public Restormer $\sigma = 50$ pretrained baseline under a unified 100-image evaluation protocol, we establish that the dominant source of improvement is the stronger trained checkpoint rather than any Test-Time wrapper.

We also report our results in the NTIRE 2026 Image Denoising Challenge (noise level = 50), where we participated under the team name **wedream**. Our submission achieved 29.89 dB PSNR and 0.87 SSIM, ranking **2nd** on the final leaderboard. This result provides an independent external validation of the effectiveness of the proposed training recipe under competitive benchmark conditions.

2. Related Work

2.1. Deep Image Denoising

Before modern transformer-based restorers, image denoising had already progressed through a long line of prior-based and convolutional methods. Classical approaches such as Non-Local Means [11], BM3D [24], and K-SVD dictionary learning [26] showed that carefully designed image priors could recover strong structure under additive noise, while trainable reaction-diffusion models [18] began to bridge model-based restoration and learned inference. Early deep restoration backbones such as MemNet [57] further confirmed that effective denoising depends not only on local filtering strength, but also on how well intermediate representations are propagated across depth.

Deep image denoising then evolved from residual CNN denoisers to more structured restoration systems. DnCNN [70] established residual learning as a strong foundation for Gaussian denoising, while FFDNet [71] introduced explicit noise-level conditioning so that one model could handle multiple noise strengths. RIDNet [7] emphasized feature attention within a single-stage design, and MPRNet [66] demonstrated that multi-stage restoration can improve difficult image recovery tasks through progressive refinement. Real-image and blind denoising work further broadened this line: CBDNet [32], CycleISP [64], the MIRNet family [65, 67], deep boosting [12], and practical blind denoisers built on data synthesis [68] all stress that realistic degradations and stronger restoration pipelines matter as much as nominal backbone size. Related formulations such as plug-and-play reconstruction with deep denoiser priors [69] also show how denoisers can serve as reusable priors beyond direct feed-forward prediction.

A second important branch studies learning without paired clean targets. Noise2Noise [36], Noise2Void [34],

Noise2Self [9], Self2Self [55], Neighbor2Neighbor [33], and high-quality self-supervised denoising [35] reveal that denoising performance can be learned from noisy observations alone under suitable independence assumptions. Adjacent temporal settings such as burst and video denoising, represented by Deep Burst Denoising [28], ViDeNN [22], and FastDVDnet [58], further highlight how extra observation diversity can compensate for harder restoration conditions.

2.2. Transformer Image Restoration

Transformer-style restoration has become a mainstream direction because long-range dependency modeling is naturally useful for image recovery. This line can be traced through generic image-processing transformers such as IPT [13] and the hierarchical Swin Transformer backbone [51], which in turn motivated restoration-oriented designs such as SwinIR [41], Uformer [62], and Restormer [63]. For the Gaussian denoising setting considered here, Restormer is already a very strong public baseline, which makes it a suitable backbone for asking a different question: how much additional performance can still be extracted without inventing a new backbone.

At the same time, the broader restoration literature continues to diversify around alternative backbone and aggregation choices. HiNet [16], NAFNet-style simple baselines [15], MAXIM [59], CAT [20], and TLC-style global information aggregation [21] each emphasize different trade-offs among efficiency, local structure modeling, and long-range interaction. More recent state-space and attention variants such as MambaIR [31], MambaIRv2 [30], ELAN [72], SRFormer [74], and activated-pixel transformer variants [17] further illustrate how image restoration continues to borrow from the wider design space of modern vision backbones.

2.3. Data-Centric Training and Test-Time Enhancement

Large and diverse image corpora are increasingly important in restoration. DIV2K [5] and Flickr2K [42] are widely used high-resolution image sources in supervised restoration, while BSD500 [8] and the Waterloo Exploration Database [52] contribute additional natural image diversity. The ESRGAN line and its OutdoorSceneTraining collection [60, 61], as well as larger-scale or officially released high-resolution sources such as LSDIR [39], DIV8K [29], LIU4K-v2 [44], and the NKUSR8K release distributed with the DiT4SR project [25], further broaden the texture coverage and spatial diversity available for restoration training. Similar data-centric observations also appear in the broader real-world and blind super-resolution literature, where realistic image sources and degradation diversity are repeatedly emphasized [14, 43].

For denoising specifically, realistic data generation, noise modeling, and benchmark construction are equally important. SIDD [3], DND [54], and RENOIR [6] provide influential real-noise benchmarks, while challenge tracks such as NTIRE 2019, 2020, and 2023 [1, 4, 40] make progress easier to compare across methods. Complementary studies on camera noise and synthesis, including cross-channel noise modeling [53], conditional noise flows [2], and unprocessing pipelines for learned raw denoising [10], reinforce the view that stronger restoration systems often emerge from stronger data assumptions as much as from stronger architectures.

Test-Time enhancement is a complementary but distinct direction. Geometric self-ensemble is widely used in restoration practice, as averaging predictions across flip and transpose transforms can reduce prediction variance with no retraining. Strong restoration baselines such as SwinIR and SRFormer explicitly report this test-time strategy [41, 74]. TLC-style global information aggregation [21] is another practical technique for improving full-image restoration behavior through local conversion. In this paper, the emphasis is not on proposing a new inference module, but on honestly separating the gains from stronger training, self-ensemble, and the retained TLC-style wrapper.

3. Method

3.1. Problem Definition and Framework Overview

We consider Gaussian color image denoising at noise level $\sigma = 50$. Let y denote the clean image and x the observed noisy image. The degradation process is

$$x = y + n, \quad n \sim \mathcal{N}(0, \sigma^2 I). \quad (1)$$

Given x , the goal is to learn a restoration function $f_\theta(\cdot)$ that produces

$$\hat{y} = f_\theta(x), \quad (2)$$

with \hat{y} as close as possible to y .

As illustrated in Figure 1, the overall framework has three components. The backbone is Restormer [63], adopted without architectural modification. The training pipeline strengthens the standard public recipe with a large-scale and diverse image corpus organized into a two-stage optimization schedule. The inference pipeline applies $\times 8$ geometric self-ensemble and retains a TLC-style local inference wrapper.

3.2. Restormer Backbone

Restormer [63] adopts a hierarchical encoder-decoder structure. The input is first mapped to feature space through overlap patch embedding, then processed by multi-scale encoder stages that progressively enlarge the receptive field. The decoder restores spatial details through upsampling and

skip connections, and a refinement module further improves the restored output. The final prediction is fused with the input through a global residual path.

Its core design combines multi-DConv head transposed attention with gated convolutional feed-forward blocks. This makes Restormer particularly suitable for high-resolution restoration because it preserves long-range context modeling while still keeping local structure sensitivity. Since the backbone is already strong, we do not alter it aggressively. Instead, the present paper concentrates on the training recipe and inference behavior wrapped around this backbone.

3.3. Large-scale Training Corpus

The public Restormer Gaussian denoising line already uses a standard multi-dataset recipe built from DIV2K [5], Flickr2K [42], BSD500 [8], and WED [52]. We strengthen this setting by explicitly shifting the focus toward larger public image diversity. The final corpus draws from seven public or officially released high-resolution image sources: DIV2K [5], Flickr2K [42], OST [60, 61], LSDIR [39], LIU4K-v2 [44], the NKUSR8K release distributed with the DiT4SR project [25], and DIV8K [29]. In practice, the ultra-high-resolution sources are first cropped into approximately 2K sub-images before patch sampling so that the training distribution remains manageable while still benefiting from richer texture statistics.

Training is organized in two stages. We start from the public Restormer $\sigma = 50$ pretrained model rather than from random initialization. In Stage I, we continue training on a base expanded corpus consisting of DIV2K [5], Flickr2K [42], OST [60, 61], and LSDIR [39]. This stage establishes a stronger and more stable restoration prior under increased scene and texture diversity. In Stage II, we further introduce LIU4K-v2 [44], the NKUSR8K release distributed with the DiT4SR project [25], and DIV8K [29], which enlarge the visual diversity and encourage broader generalization. Across both stages, the main point is not merely to use more data, but to obtain a stronger final checkpoint through a more capable data recipe. After combining the two stages, the overall training pool contains seven sources and 143,679 images.

To keep the presentation compact, we summarize the full recipe in one table instead of keeping separate dataset and optimizer tables. Both stages use AdamW and MSE loss on $4 \times$ NVIDIA H200 GPUs, while the learning rate drops from 1×10^{-4} in Stage I to 1×10^{-5} in Stage II.

3.4. Test-Time Enhancement

Geometric self-ensemble. Although a single forward pass already produces a strong result, neural denoisers are not strictly invariant to flips and transposes. This motivates $\times 8$ geometric self-ensemble, a test-time strategy explicitly

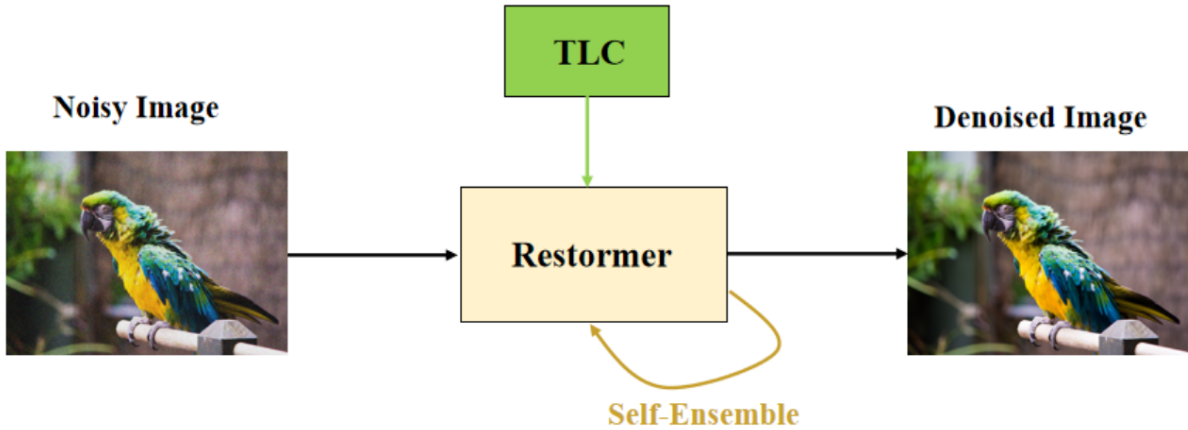


Figure 1. Overview of the final denoising pipeline. A noisy image is restored by Restormer, the TLC-style wrapper is retained for inference consistency, and $\times 8$ self-ensemble is used to refine the final denoised output.

Table 1. Two-stage training summary.

Item	Stage I	Stage II
Data	DIV2K / Flickr2K / OST / LSDIR	Stage I + LIU4K-v2 / NKUSR8K / DIV8K
Patch	256 \rightarrow 448 \rightarrow 768	768
Batch	4 \rightarrow 2 \rightarrow 1	4
Iterations	300K	300K
Initial LR	1×10^{-4}	1×10^{-5}
Goal	Stable restoration prior	Broader texture diversity

used in strong restoration baselines such as SwinIR and SRFormer [41, 74]. Let $T_k(\cdot)$ denote the k -th geometric transform. The final prediction is

$$\hat{y} = \frac{1}{K} \sum_{k=1}^K T_k^{-1}(f_{\theta}(T_k(x))), \quad K = 8. \quad (3)$$

This strategy does not change the model parameters or training cost, but increases inference time by about a factor of eight. It is therefore a typical accuracy-through-computation trade-off.

TLC-style local inference wrapper. The final implementation also keeps a TLC-style local inference wrapper [21]. Importantly, this wrapper is not treated as a new independently trained backbone. It is a deployment-level wrapper around the same Restormer weights, kept mainly for implementation consistency and local inference adaptation. The experiments later show that its measurable quantitative effect is negligible in the current Gaussian denoising setting, so it should not be interpreted as the dominant source of the final performance gain.

3.5. Final Inference Pipeline

The final inference pipeline is straightforward. A three-channel noisy RGB input is first cropped to a spatial size divisible by eight. The image is then normalized to the $[0, 1]$ range and converted to tensor form. The TLC-style wrapped Restormer backbone [21, 63] restores the image, optionally under the eight geometric transforms used for self-ensemble. The predictions are mapped back to the RGB image space after inverse transformation and averaging. Clean reference images are only used for metric computation, not as inputs to the model.

4. Experiments

4.1. Experimental Settings

Training follows the expanded public corpus and two-stage strategy described in Section 3. Validation is performed on a unified 100-image protocol, and PSNR and SSIM are the main evaluation metrics. Unless otherwise stated, the main reported system is the TLC-style wrapped Restormer with $\times 8$ self-ensemble.

The experiments are organized to isolate the true source of improvement. We first report the main final result under the unified protocol. We then study the influence of self-ensemble and the TLC-style wrapper through inference ablation. After that, we compare checkpoints from different training stages to examine parameter evolution. Finally, we compare the resulting model with the public Restormer $\sigma = 50$ pretrained baseline under the same protocol, while the deployment cost is discussed directly from the same ablation table instead of a separate efficiency table.

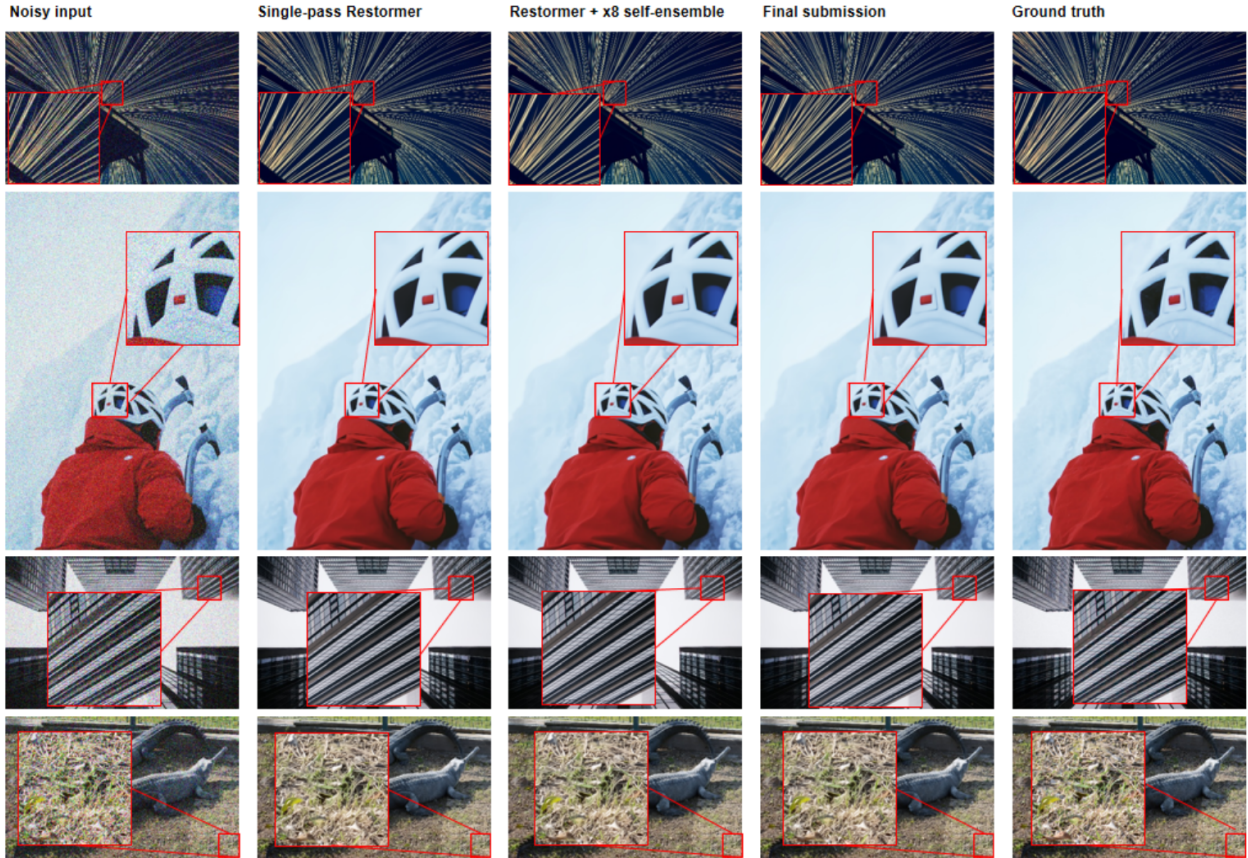


Figure 2. Qualitative comparison among the noisy input, single-pass Restormer, Restormer with $\times 8$ self-ensemble, final submission, and ground truth. The largest visual gains appear in line-rich, structured, and texture-dense regions.

4.2. Main Result

The final wrapped system with $\times 8$ self-ensemble reaches 30.7622 dB PSNR and 0.8607 SSIM, with average inference time 8815.73 ms and peak memory 36956 MB on the unified 100-image validation set. Because these final numbers are already covered again in the same-protocol baseline comparison, we report them here directly in text instead of keeping a separate one-row table. This confirms that the strengthened training-and-inference recipe consistently yields strong Gaussian denoising performance under one unified protocol.

4.3. Inference Ablation

Table 2 restores the full four-way inference ablation from the source draft. The most stable finding is that geometric self-ensemble provides a small but consistent gain regardless of whether the TLC-style wrapper is enabled. By contrast, the wrapper itself contributes almost nothing measurable in this task.

The gain from self-ensemble is about 0.0273 dB PSNR and 0.0004 SSIM, which is small but stable. The wrapped

Table 2. Inference ablation under the unified 100-image protocol.

Variant	PSNR	SSIM	Time/ms	Mem/MB
Restormer, 1-pass	30.7349	0.8603	1063.01	36089
Restormer, $\times 8$	30.7622	0.8607	8759.55	36856
Wrapped, 1-pass	30.7349	0.8603	1053.60	36190
Wrapped, $\times 8$	30.7622	0.8607	8815.73	36956

and unwrapped variants are numerically almost identical. This supports the central interpretation of the paper: the dominant inference-side gain comes from self-ensemble, while the TLC-style wrapper is not the main reason for the final improvement.

4.4. Checkpoint Evolution

To understand how much of the improvement comes from the final training stage, we directly compare an earlier checkpoint with the final model in text rather than keeping a separate low-yield table. Intermediate checkpoint A (about 200K iterations) reaches 30.7580 dB PSNR and 0.8606 SSIM, while the final model reaches 30.7622 dB and 0.8607. The gap is therefore only about 0.0042 dB PSNR

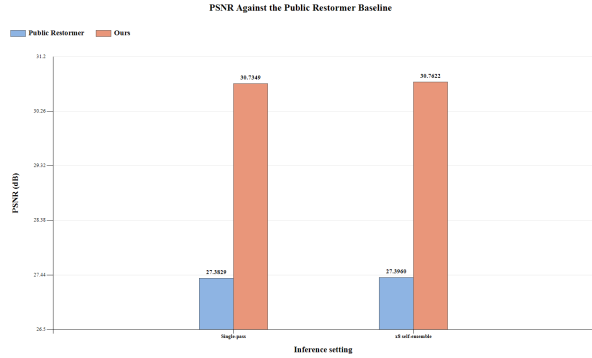


Figure 3. Same-protocol PSNR comparison with the public Restormer $\sigma = 50$ pretrained baseline. The gap remains large in both the single-pass and $\times 8$ self-ensemble settings; the corresponding SSIM gains are $+0.0737$ in both cases.

and 0.0001 SSIM, suggesting that training had already converged strongly before the final stage ended.

4.5. Comparison with the Restormer Baseline

Figure 3 converts the same-protocol baseline comparison into a compact visual summary. The performance gap is already large in the single-pass setting, and self-ensemble only adds a relatively small additional improvement on top of that stronger checkpoint. Quantitatively, the PSNR margin is $+3.3520$ dB for single-pass inference and $+3.3662$ dB with $\times 8$ self-ensemble, while the SSIM gain remains $+0.0737$ in both settings. This again suggests that the major gain comes from stronger checkpoints learned from the expanded training corpus rather than from the wrapper alone.

4.6. Efficiency and Visual Discussion

As shown in Table 2, on the wrapped path, $\times 8$ self-ensemble increases average inference time from 1053.60 ms to 8815.73 ms and raises peak memory from 36190 MB to 36956 MB. The unwrapped path shows the same pattern, confirming that the final gain is real but computation-heavy.

The qualitative observations are also image-dependent. As shown in Figure 2, self-ensemble is most helpful in texture-rich and regular-structure regions. In the source draft, sample 0828 gains 0.2463 dB PSNR in a high-frequency line region, and sample 0845 gains 0.1163 dB on a structured texture example. By contrast, the gains shrink noticeably in smoother or more ambiguous regions: samples 0844 and 0895 improve by only 0.0328 dB and 0.0084 dB, respectively. This indicates that self-ensemble should be viewed as a gradual robustness refinement rather than as a uniformly large structural improvement.

Taken together, Table 2 and Figures 3 and Figures 2 make the precision-efficiency trade-off explicit. If the goal is to obtain the strongest final restoration quality, keeping

$\times 8$ self-ensemble is reasonable. If throughput or deployment cost matters more, single-pass inference already provides strong and stable restoration quality.

5. Conclusion

This paper presents a Restormer-based Gaussian color image denoising pipeline built around an expanded public training corpus and self-ensemble inference. Instead of re-designing the backbone, the method strengthens the final checkpoint through a data-centric two-stage recipe and then releases a small but stable extra gain through $\times 8$ geometric self-ensemble. On the unified 100-image validation protocol, the final model reaches 30.7622 dB PSNR and 0.8607 SSIM, and improves over the public Restormer $\sigma = 50$ pretrained baseline by up to 3.3662 dB PSNR under the same protocol.

References

- [1] Abdelrahman Abdelhamed, Mahmoud Afifi, Radu Timofte, Michael S. Brown, et al. NTIRE 2020 challenge on real image denoising: Dataset, methods and results. In *Proceedings of the IEEE/CVF Conference on Computer Vision and Pattern Recognition Workshops*, pages 2077–2088, 2020. 3
- [2] Abdelrahman Abdelhamed, Marcus A Brubaker, and Michael S Brown. Noise Flow: Noise modeling with conditional normalizing flows. In *Proceedings of the IEEE/CVF International Conference on Computer Vision*, pages 3165–3173, 2019. 3
- [3] Abdelrahman Abdelhamed, Stephen Lin, and Michael S Brown. A high-quality denoising dataset for smartphone cameras. In *Proceedings of the IEEE Conference on Computer Vision and Pattern Recognition*, pages 1692–1700, 2018. 3
- [4] Abdelrahman Abdelhamed, Radu Timofte, Michael S. Brown, et al. NTIRE 2019 challenge on real image denoising: Methods and results. In *Proceedings of the IEEE/CVF Conference on Computer Vision and Pattern Recognition Workshops*, pages 2197–2210, 2019. 3
- [5] Eirikur Agustsson and Radu Timofte. NTIRE 2017 challenge on single image super-resolution: Dataset and study. In *Proceedings of the IEEE Conference on Computer Vision and Pattern Recognition Workshops*, pages 126–135, 2017. 2, 3
- [6] Josue Anaya and Adrian Barbu. RENOIR—a dataset for real low-light image noise reduction. *Journal of Visual Communication and Image Representation*, 51:144–154, 2018. 3
- [7] Saeed Anwar and Nick Barnes. Real image denoising with feature attention. In *Proceedings of the IEEE/CVF International Conference on Computer Vision*, pages 3155–3164, 2019. 1, 2
- [8] Pablo Arbeláez, Michael Maire, Charless Fowlkes, and Jitendra Malik. Contour detection and hierarchical image segmentation. *IEEE Transactions on Pattern Analysis and Machine Intelligence*, 33(5):898–916, 2011. 2, 3

- [9] Joshua Batson and Loic Royer. Noise2Self: Blind denoising by self-supervision. In *Proceedings of the International Conference on Machine Learning*, pages 524–533. PMLR, 2019. 2
- [10] Tim Brooks, Ben Mildenhall, Tianfan Xue, Jiawen Chen, Dillon Sharlet, and Jonathan T Barron. Unprocessing images for learned raw denoising. In *Proceedings of the IEEE/CVF Conference on Computer Vision and Pattern Recognition*, pages 11036–11045, 2019. 3
- [11] Antoni Buades, Bartomeu Coll, and J-M Morel. A non-local algorithm for image denoising. In *Proceedings of the 2005 IEEE Computer Society Conference on Computer Vision and Pattern Recognition (CVPR'05)*, volume 2, pages 60–65. IEEE, 2005. 2
- [12] Chang Chen, Zhiwei Xiong, Xinmei Tian, Zheng-Jun Zha, and Feng Wu. Real-world image denoising with deep boosting. *IEEE Transactions on Pattern Analysis and Machine Intelligence*, 42(12):3071–3087, 2019. 2
- [13] Hanting Chen, Yunhe Wang, Tianyu Guo, Chang Xu, Yiping Deng, Zhenhua Liu, Siwei Ma, Chunjing Xu, Chao Xu, and Wen Gao. Pre-trained image processing transformer. In *Proceedings of the IEEE/CVF Conference on Computer Vision and Pattern Recognition*, pages 12299–12310, 2021. 2
- [14] Honggang Chen, Xiaohai He, Linbo Qing, Yuanyuan Wu, Chao Ren, Ray E Sheriff, and Ce Zhu. Real-world single image super-resolution: A brief review. *Information Fusion*, 79:124–145, 2022. 2
- [15] Liangyu Chen, Xiaojie Chu, Xiangyu Zhang, and Jian Sun. Simple baselines for image restoration. In *Proceedings of the European Conference on Computer Vision (ECCV)*, pages 17–33. Springer, 2022. 2
- [16] Liangyu Chen, Xin Lu, Jie Zhang, Xiaojie Chu, and Chengpeng Chen. HiNet: Half instance normalization network for image restoration. In *Proceedings of the IEEE/CVF Conference on Computer Vision and Pattern Recognition*, pages 182–192, 2021. 2
- [17] Xiangyu Chen, Xintao Wang, Jiantao Zhou, Yu Qiao, and Chao Dong. Activating more pixels in image super-resolution transformer. In *Proceedings of the IEEE/CVF Conference on Computer Vision and Pattern Recognition*, pages 22367–22377, 2023. 2
- [18] Yunjin Chen and Thomas Pock. Trainable nonlinear reaction diffusion: A flexible framework for fast and effective image restoration. *IEEE Transactions on Pattern Analysis and Machine Intelligence*, 39(6):1256–1272, 2016. 2
- [19] Zheng Chen, Kai Liu, Jingkai Wang, Xianglong Yan, Jianze Li, Ziqing Zhang, Jue Gong, Jiatong Li, Lei Sun, Xiaoyang Liu, Radu Timofte, Yulun Zhang, et al. The fourth challenge on image super-resolution ($\times 4$) at NTIRE 2026: Benchmark results and method overview. In *Proceedings of the Computer Vision and Pattern Recognition Conference Workshops*, 2026.
- [20] Zheng Chen, Yulun Zhang, Jinjin Gu, Linghe Kong, Xin Yuan, et al. Cross aggregation transformer for image restoration. *Advances in Neural Information Processing Systems*, 35:25478–25490, 2022. 2
- [21] Xiaojie Chu, Liangyu Chen, Chengpeng Chen, and Xin Lu. Improving image restoration by revisiting global information aggregation. In *Proceedings of the European Conference on Computer Vision (ECCV)*, pages 53–71. Springer, 2022. 2, 3, 4
- [22] Michele Claus and Jan Van Gemert. ViDeNN: Deep blind video denoising. In *Proceedings of the IEEE/CVF Conference on Computer Vision and Pattern Recognition Workshops*, pages 0–0, 2019. 2
- [23] Ziteng Cui, Shuhong Liu, Xiaoyu Dong, Xuangeng Chu, Lin Gu, Ming-Hsuan Yang, and Tatsuya Harada. Unifying color and lightness correction with view-adaptive curve adjustment for robust 3d novel view synthesis. *arXiv preprint arXiv:2602.18322*, 2026. 1
- [24] Kostadin Dabov, Alessandro Foi, Vladimir Katkovnik, and Karen Egiazarian. Image denoising by sparse 3-d transform-domain collaborative filtering. *IEEE Transactions on Image Processing*, 16(8):2080–2095, 2007. 2
- [25] Zheng-Peng Duan, Jiawei Zhang, Xin Jin, Ziheng Zhang, Zheng Xiong, Dongqing Zou, Jimmy S. Ren, Chun-Le Guo, and Chongyi Li. NKUSR8K: dataset release in the official DiT4SR project repository. Official project repository, 2025. Repository documentation states that the NKUSR8K dataset is released for training with the DiT4SR project. 2, 3
- [26] Michael Elad and Michal Aharon. Image denoising via sparse and redundant representations over learned dictionaries. *IEEE Transactions on Image Processing*, 15(12):3736–3745, 2006. 2
- [27] Xining Ge, Weijun Yuan, Gengjia Chang, Xuyang Li, and Shuhong Liu. Clip-guided data augmentation for night-time image dehazing. *arXiv preprint arXiv:2604.05500*, 2026. 1
- [28] Clément Godard, Kevin Matzen, and Matt Uyttendaele. Deep burst denoising. In *Proceedings of the European Conference on Computer Vision (ECCV)*, pages 538–554, 2018. 2
- [29] Shuhang Gu, Andreas Lugmayr, Martin Danelljan, Manuel Fritsche, Julien Lamour, and Radu Timofte. DIV8K: DIVERse 8k resolution image dataset. In *Proceedings of the IEEE/CVF International Conference on Computer Vision Workshops*, pages 3512–3516. IEEE, 2019. 2, 3
- [30] Hang Guo, Yong Guo, Yaohua Zha, Yulun Zhang, Wenbo Li, Tao Dai, Shu-Tao Xia, and Yawei Li. MambaIRv2: Attentive state space restoration. In *Proceedings of the IEEE/CVF Conference on Computer Vision and Pattern Recognition*, pages 28124–28133, 2025. 2
- [31] Hang Guo, Jinmin Li, Tao Dai, Zhihao Ouyang, Xudong Ren, and Shu-Tao Xia. MambaIR: A simple baseline for image restoration with state-space model. In *Proceedings of the European Conference on Computer Vision (ECCV)*, pages 222–241. Springer, 2024. 2
- [32] Shi Guo, Zifei Yan, Kai Zhang, Wangmeng Zuo, and Lei Zhang. Toward convolutional blind denoising of real photographs. In *Proceedings of the IEEE/CVF Conference on Computer Vision and Pattern Recognition*, pages 1712–1722, 2019. 2
- [33] Tao Huang, Songjiang Li, Xu Jia, Huchuan Lu, and Jianzhuang Liu. Neighbor2Neighbor: Self-supervised denoising from single noisy images. In *Proceedings of the IEEE/CVF Conference on Computer Vision and Pattern Recognition*, pages 14781–14790, 2021. 2

- [34] Alexander Krull, Tim-Oliver Buchholz, and Florian Jug. Noise2Void: Learning denoising from single noisy images. In *Proceedings of the IEEE/CVF Conference on Computer Vision and Pattern Recognition*, pages 2129–2137, 2019. 2
- [35] Samuli Laine, Tero Karras, Jaakko Lehtinen, and Timo Aila. High-quality self-supervised deep image denoising. *Advances in Neural Information Processing Systems*, 32, 2019. 2
- [36] Jaakko Lehtinen, Jacob Munkberg, Jon Hasselgren, Samuli Laine, Tero Karras, Miika Aittala, and Timo Aila. Noise2Noise: Learning image restoration without clean data. In *Proceedings of the 35th International Conference on Machine Learning*, volume 80 of *Proceedings of Machine Learning Research*, pages 2965–2974. PMLR, 2018. 2
- [37] Mingrui Li, Shuhong Liu, Tianchen Deng, and Hongyu Wang. Densesplat: Densifying gaussian splatting slam with neural radiance prior. *IEEE Transactions on Visualization & Computer Graphics*, (01):1–14, 2025. 1
- [38] Mingrui Li, Shuhong Liu, Heng Zhou, Guohao Zhu, Na Cheng, Tianchen Deng, and Hongyu Wang. Sgs-slam: Semantic gaussian splatting for neural dense slam. In *European Conference on Computer Vision*, pages 163–179, 2025. 1
- [39] Yawei Li, Kai Zhang, Jingyun Liang, Jiezhong Cao, Ce Liu, Rui Gong, Yulun Zhang, Hao Tang, Yun Liu, Denis Demandolx, et al. LSDIR: A large-scale dataset for image restoration. In *Proceedings of the IEEE/CVF Conference on Computer Vision and Pattern Recognition*, pages 1775–1787, 2023. 2, 3
- [40] Yawei Li, Yulun Zhang, Radu Timofte, Luc Van Gool, Zhi-jun Tu, Kunpeng Du, Hailing Wang, Hanting Chen, Wei Li, Xiaofei Wang, et al. Ntire 2023 challenge on image denoising: Methods and results. In *Proceedings of the IEEE/CVF Conference on Computer Vision and Pattern Recognition*, pages 1905–1921, 2023. 3
- [41] Jingyun Liang, Jiezhong Cao, Guolei Sun, Kai Zhang, Luc Van Gool, and Radu Timofte. SwinIR: Image restoration using Swin Transformer. In *Proceedings of the IEEE/CVF International Conference on Computer Vision*, pages 1833–1844, 2021. 1, 2, 3, 4
- [42] Bee Lim, Sanghyun Son, Heewon Kim, Seungjun Nah, and Kyoung Mu Lee. Flickr2K dataset. Official dataset release accompanying the NTIRE2017/EDSR repository, 2017. Dataset collected by the authors using the Flickr API. 2, 3
- [43] Anran Liu, Yihao Liu, Jinjin Gu, Yu Qiao, and Chao Dong. Blind image super-resolution: A survey and beyond. *IEEE Transactions on Pattern Analysis and Machine Intelligence*, 45(5):5461–5480, 2022. 2
- [44] Jiaying Liu, Dong Liu, Wenhan Yang, Sifeng Xia, Xiaoshuai Zhang, and Yuanying Dai. LIU4K-v2 dataset. Official dataset page, 2020. The official LIU4K-v2 page recommends citing the accompanying compression artifact reduction benchmark paper. 2, 3
- [45] Shuhong Liu, Chenyu Bao, Ziteng Cui, Xuangeng Chu, Bin Ren, Lin Gu, Xiang Chen, Mingrui Li, Long Ma, Marcos V. Conde, Radu Timofte, et al. NTIRE 2026 3D restoration and reconstruction in adverse conditions: RealX3D challenge results. *arXiv preprint arXiv:2604.04135*, 2026. 1
- [46] Shuhong Liu, Chenyu Bao, Ziteng Cui, Yun Liu, Xuangeng Chu, Lin Gu, Marcos V Conde, Ryo Umagami, Tomohiro Hashimoto, Zijian Hu, et al. Realx3d: A physically-degraded 3d benchmark for multi-view visual restoration and reconstruction. *arXiv preprint arXiv:2512.23437*, 2026. 1
- [47] Shuhong Liu, Xiang Chen, Hongming Chen, Quanfeng Xu, and Mingrui Li. Deraings: Gaussian splatting for enhanced scene reconstruction in rainy environments. *Proceedings of the AAAI Conference on Artificial Intelligence*, 39(5):5558–5566, 2025. 1
- [48] Shuhong Liu, Tianchen Deng, Heng Zhou, Liuzhuozheng Li, Hongyu Wang, Danwei Wang, and Mingrui Li. Mg-slam: Structure gaussian splatting slam with manhattan world hypothesis. *IEEE Transactions on Automation Science and Engineering*, 22:17034–17049, 2025. 1
- [49] Shuhong Liu, Xining Ge, Ziying Gu, Lin Gu, Ziteng Cui, Xuangeng Chu, Jun Liu, Dong Li, and Tatsuya Harada. Denoising the deep sky: Physics-based ccd noise formation for astronomical imaging. *arXiv preprint arXiv:2601.23276*, 2026. 1
- [50] Shuhong Liu, Lin Gu, Ziteng Cui, Xuangeng Chu, and Tatsuya Harada. I2-nerf: Learning neural radiance fields under physically-grounded media interactions. In *Advances in Neural Information Processing Systems*, 2025. 1
- [51] Ze Liu, Yutong Lin, Yue Cao, Han Hu, Yixuan Wei, Zheng Zhang, Stephen Lin, and Baining Guo. Swin Transformer: Hierarchical vision transformer using shifted windows. In *Proceedings of the IEEE/CVF International Conference on Computer Vision*, pages 10012–10022, 2021. 2
- [52] Kede Ma, Zhengfang Duanmu, Qingbo Wu, Zhou Wang, Hongwei Yong, Hongliang Li, and Lei Zhang. Waterloo Exploration Database: New challenges for image quality assessment models. *IEEE Transactions on Image Processing*, 26(2):1004–1016, 2017. 2, 3
- [53] Seonghyeon Nam, Youngbae Hwang, Yasuyuki Matsushita, and Seon Joo Kim. A holistic approach to cross-channel image noise modeling and its application to image denoising. In *Proceedings of the IEEE Conference on Computer Vision and Pattern Recognition*, pages 1683–1691, 2016. 3
- [54] Tobias Plotz and Stefan Roth. Benchmarking denoising algorithms with real photographs. In *Proceedings of the IEEE Conference on Computer Vision and Pattern Recognition*, pages 1586–1595, 2017. 3
- [55] Yuhui Quan, Mingqin Chen, Tongyao Pang, and Hui Ji. Self2Self with dropout: Learning self-supervised denoising from single image. In *Proceedings of the IEEE/CVF Conference on Computer Vision and Pattern Recognition*, pages 1890–1898, 2020. 2
- [56] Bin Ren, Hang Guo, Yan Shu, Jiaqi Ma, Ziteng Cui, Shuhong Liu, Guofeng Mei, Lei Sun, Zongwei Wu, Fahad Shahbaz Khan, Salman Khan, Radu Timofte, Yawei Li, et al. The eleventh NTIRE 2026 efficient super-resolution challenge report. *arXiv preprint arXiv:2604.03198*, 2026. 1
- [57] Ying Tai, Jian Yang, Xiaoming Liu, and Chunyan Xu. MemNet: A persistent memory network for image restoration. In

- Proceedings of the IEEE International Conference on Computer Vision*, pages 4539–4547, 2017. 2
- [58] Matias Tassano, Julie Delon, and Thomas Veit. FastDVDnet: Towards real-time deep video denoising without flow estimation. In *Proceedings of the IEEE/CVF Conference on Computer Vision and Pattern Recognition*, pages 1354–1363, 2020. 2
- [59] Zhengzhong Tu, Hossein Talebi, Han Zhang, Feng Yang, Peyman Milanfar, Alan Bovik, and Yinxiao Li. MAXIM: Multi-axis MLP for image processing. In *Proceedings of the IEEE/CVF Conference on Computer Vision and Pattern Recognition*, pages 5769–5780, 2022. 2
- [60] Xintao Wang, Ke Yu, Chao Dong, and Chen Change Loy. Recovering realistic texture in image super-resolution by deep spatial feature transform. In *Proceedings of the IEEE Conference on Computer Vision and Pattern Recognition*, pages 606–615, 2018. 2, 3
- [61] Xintao Wang, Ke Yu, Shixiang Wu, Jinjin Gu, Yihao Liu, Chao Dong, Yu Qiao, and Chen Change Loy. ESRGAN: Enhanced super-resolution generative adversarial networks. In *Proceedings of the European Conference on Computer Vision Workshops*, 2018. 2, 3
- [62] Zhendong Wang, Xiaodong Cun, Jianmin Bao, Wengang Zhou, Jianzhuang Liu, and Houqiang Li. Uformer: A general u-shaped transformer for image restoration. In *Proceedings of the IEEE/CVF Conference on Computer Vision and Pattern Recognition*, pages 17683–17693, 2022. 1, 2
- [63] Syed Waqas Zamir, Aditya Arora, Salman Khan, Munawar Hayat, Fahad Shahbaz Khan, and Ming-Hsuan Yang. Restormer: Efficient transformer for high-resolution image restoration. In *Proceedings of the IEEE/CVF Conference on Computer Vision and Pattern Recognition*, pages 5728–5739, 2022. 1, 2, 3, 4
- [64] Syed Waqas Zamir, Aditya Arora, Salman Khan, Munawar Hayat, Fahad Shahbaz Khan, Ming-Hsuan Yang, and Ling Shao. CycleISP: Real image restoration via improved data synthesis. In *Proceedings of the IEEE/CVF Conference on Computer Vision and Pattern Recognition*, pages 2696–2705, 2020. 2
- [65] Syed Waqas Zamir, Aditya Arora, Salman Khan, Munawar Hayat, Fahad Shahbaz Khan, Ming-Hsuan Yang, and Ling Shao. Learning enriched features for real image restoration and enhancement. In *Proceedings of the European Conference on Computer Vision (ECCV)*, pages 492–511. Springer, 2020. 2
- [66] Syed Waqas Zamir, Aditya Arora, Salman Khan, Munawar Hayat, Fahad Shahbaz Khan, Ming-Hsuan Yang, and Ling Shao. Multi-stage progressive image restoration. In *Proceedings of the IEEE/CVF Conference on Computer Vision and Pattern Recognition*, pages 14821–14831, 2021. 1, 2
- [67] Syed Waqas Zamir, Aditya Arora, Salman Khan, Munawar Hayat, Fahad Shahbaz Khan, Ming-Hsuan Yang, and Ling Shao. Learning enriched features for fast image restoration and enhancement. *IEEE Transactions on Pattern Analysis and Machine Intelligence*, 45(2):1934–1948, 2022. 2
- [68] Kai Zhang, Yawei Li, Jingyun Liang, Jie Zhang Cao, Yulun Zhang, Hao Tang, Deng-Ping Fan, Radu Timofte, and Luc Van Gool. Practical blind image denoising via Swin-Conv-UNet and data synthesis. *Machine Intelligence Research*, 20(6):822–836, 2023. 2
- [69] Kai Zhang, Yawei Li, Wangmeng Zuo, Lei Zhang, Luc Van Gool, and Radu Timofte. Plug-and-play image restoration with deep denoiser prior. *IEEE Transactions on Pattern Analysis and Machine Intelligence*, 44(10):6360–6376, 2021. 2
- [70] Kai Zhang, Wangmeng Zuo, Yunjin Chen, Deyu Meng, and Lei Zhang. Beyond a gaussian denoiser: Residual learning of deep CNN for image denoising. *IEEE Transactions on Image Processing*, 26(7):3142–3155, 2017. 1, 2
- [71] Kai Zhang, Wangmeng Zuo, and Lei Zhang. FFDNet: Toward a fast and flexible solution for CNN-based image denoising. *IEEE Transactions on Image Processing*, 27(9):4608–4622, 2018. 1, 2
- [72] Xindong Zhang, Hui Zeng, Shi Guo, and Lei Zhang. Efficient long-range attention network for image super-resolution. In *Proceedings of the European Conference on Computer Vision (ECCV)*, pages 649–667. Springer, 2022. 2
- [73] Heng Zhou, Zhetao Guo, Yuxiang Ren, Shuhong Liu, Lechen Zhang, Kaidi Zhang, and Mingrui Li. Modslam: Monocular dense mapping for unbounded 3d scene reconstruction. *IEEE Robotics and Automation Letters*, 10(1):484–491, 2024. 1
- [74] Yupeng Zhou, Zhen Li, Chun-Le Guo, Song Bai, Ming-Ming Cheng, and Qibin Hou. SRFormer: Permuted self-attention for single image super-resolution. In *Proceedings of the IEEE/CVF International Conference on Computer Vision*, pages 12780–12791, 2023. 2, 3, 4